한국액체미립화학회지 제21권 제4호(2016)
http://dx.doi.org/10.15435/JILASSKR.2016.21.4.184

Development of Two-color Radiation Thermometer for Harsh Environments

Mohammed Ali Alshaikh Mohammed* and Kim Ki-Seong†

Key Words: Temperature measurement, Radiation thermometer, Harsh environment

Abstract

Many industrial processes require reliable temperature measurements in harsh environments with high temperature, dust, humidity, and pressure. However, commercially-available conventional temperature measurement devices are not suitable for use in such conditions. This study thus proposes a reliable, durable two-color radiation thermometer (RT) for harsh environments that was developed by selecting the appropriate components, designing a suitable mechanical structure, and compensating environmental factors such as absorption by particles and gases. The two-color RT has a simple, compactly-designed probe with a well-structured data acquisition system combined with efficient LabVIEW-based code. As a result, the RT can measure the temperature in real time, ranging from 300 to 900°C in extremely harsh environments, such as that above the burden zone of a blast furnace. The error in the temperature measurements taken with the proposed two-color RT compared to that obtained using K-type thermocouple readouts was within 6.1 to 1.4°C at a temperature range from 200 to 700°C. The effects of absorption by gases including CO_2, CO and H_2O and the scattering by fine particles were calculated to find the transmittance of the two wavelength bands of operation through the path between the measured burden surface and the two-color probe. This method is applied to determine the transmittance of the short and long wavelength bands to be 0.31 and 0.51, respectively. Accordingly, the signals that were measured were corrected, and the true burden surface temperature was calculated. The proposed two-color RT and the correction method can be applied to measure temperatures in harsh environments where light-absorbing gases and scattering particles exist and optical components can be contaminated.

1. Introduction

In many industrial applications, real-time temperature measurements play an important role in improving product quality, reducing operating costs, and ensuring safety[1].

The majority of commercially existing temperature measurement devices are made using thermocouples, RTDs and RTs. These conventional devices have been in use for several decades. However, due to the harsh environment suffering high temperature, dust, hot gases and high pressure, such as in blast furnace for pig iron production, commercially available temperature measurement devices are not applicable, or the performances achievable by these conventional devices regarding their sensitivity, accuracy and durability[2,3].

Several approaches for measuring temperature in such environments have been studied in the past [4-8]. One such method is to implement two-color radiation thermometry, which is a non-contact method that can measure the temperature of inaccessible objects, moving objects, and objects with changing emissivities[1,9-11].

However, a two-color radiation thermometer (RT) must operate in atmospheric windows with a high atmospheric transmission, and it is difficult to employ these as durable and reliable temperature measure-

(Recieved: 12 Oct 2016, Recieved in revised form: 17 Nov 2016, Accepted: 18 Nov 2016)
*Central laboratory, Ministry of High Education and Scientific Research, P.O Box 7099, Khartoum, Sudan
†책임저자, 종신회원, 전남대학교 기계설계공학부
E-mail : m.a.elshaikh@gmail.com, sngkim@chonnam.ac.kr
TEL : (043)261-2583 FAX : (043)271-4413

ment devices in some cases with harsh measurement environments because the thermal radiation emitted by the measured object is continuously influenced by the environment itself[3]. Thermal radiation is absorbed and scattered in some wavelengths over a wide temperature range due to the presence of CO_2, water vapor and hydrocarbons. Particulates such as pulverized coal in a furnace, soot, dust, and aerosol in the atmosphere also scatter and absorb thermal radiation[12]. Thus, the effect of the measurement environment on the thermal radiation of the object at different wavelengths should be considered to reliably measure the temperature, and corrections should be made to minimize or eliminate the effect of such environment.

Additionally, conventional RTs are not viable for use under harsh measurement conditions due to their sensitivity and durability.

Recently, the demand has increased for reliable, durable RT devices tailored to measure the temperature in harsh conditions, and such applications also demand automated RTs comprised of a compact probe coupled with efficient software and reliable error-correction.

The objective of the current study is to investigate the feasibility of developing a remote-controlled two-color RT with reasonable accuracy and a fast response to measure the temperature of objects with unknown emissivity located in a harsh environment.

2. Theoretical Background

The proposed two-color RT operates according to Planck's law[13]. This law states that the spectral radiance (S) of the thermal radiation emitted from an object when its temperature is above absolute zero is a function of the object temperature (T) and the thermal radiation wavelength (λ). For a blackbody, Wien's approximation describes the relationship between S, T, and λ as follows:

$$S_{b,\lambda}(\lambda,T) = C_1\lambda^{-5}e^{-\frac{C_2}{\lambda T}} \tag{1}$$

where, C_1 is the first radiation constant, $C_1 = 2\pi hc^2$, where, h is Planck's constant, c is the speed of light in vacuum. While, C_2 is the second radiation constant, $C_2 = hc/k$. where, k is Boltzmann's constant.

In accordance with Eq. (1) the intensities, $I_{\lambda1}$ and $I_{\lambda2}$, of the thermal radiance at the two wavelengths, λ_1 and λ_2, represent the intensities of the two-color bands and can be given by Eq. (2) and Eq. (3) as follows:

$$I_{\lambda1}(T) = KC_1\varepsilon_{\lambda1}\lambda_1^{-5}e^{-\frac{C_2}{\lambda_1 T}} \tag{2}$$

$$I_{\lambda2}(T) = KC_1\varepsilon_{\lambda2}\lambda_2^{-5}e^{-\frac{C_2}{\lambda_2 T}} \tag{3}$$

where, K is the device factor that depends on the geometrical design of the device and the component specification[3,15].

Then, the ratio (R) between $I_{\lambda2}$ and $I_{\lambda1}$ can be given as follows:

$$R = \frac{I_{\lambda2}(T)}{I_{\lambda1}(T)} = \frac{\lambda_1^5\varepsilon_{\lambda2}}{\lambda_2^5\varepsilon_{\lambda1}}e^{-\frac{C_2}{T}\left[\frac{1}{\lambda_2}-\frac{1}{\lambda_1}\right]} \tag{4}$$

The temperature (T) in Eq. (4) is known as the ratio temperature (T_{ratio})

$$\frac{1}{T_{ratio}} = \frac{lnR - ln\frac{\lambda_1^5}{\lambda_2^5} - ln\frac{\varepsilon_{\lambda2}}{\varepsilon_{\lambda1}}}{-C_2\left[\frac{1}{\lambda_2}-\frac{1}{\lambda_1}\right]} \tag{5}$$

For a blackbody, the ratio is given by:

$$R_b = \frac{I_{\lambda2}(T)}{I_{\lambda1}(T)} = \frac{\lambda_1^5}{\lambda_2^5}e^{-\frac{C_2}{T}\left[\frac{1}{\lambda_2}-\frac{1}{\lambda_1}\right]} \tag{6}$$

The temperature (T) in Eq. (6) is the true temperature (T_{true})

$$\frac{1}{T_{true}} = \frac{lnR - ln\frac{\lambda_1^5}{\lambda_2^5}}{-C_2\left[\frac{1}{\lambda_2}-\frac{1}{\lambda_1}\right]} \tag{7}$$

From Eq. (5) and Eq. (7)

$$\frac{1}{T_{ratio}} = \frac{1}{T_{rrue}} - \frac{\ln\left(\frac{\varepsilon_{\lambda2}}{\varepsilon_{\lambda1}}\right)}{-C_2\left[\frac{1}{\lambda_2}-\frac{1}{\lambda_1}\right]} \tag{8}$$

If $\varepsilon_{\lambda 1}$ and $\varepsilon_{\lambda 2}$ are equal, then $T_{ratio} = T_{true}$

The main advantage of this method is that the temperature is measured independently of the emissivity, and the main source of error occurs when the measured object does not behave like a gray body[14,15]. In addition, the two-color RTs can also be subjected sources due to a limited atmospheric transmittance, differences in the radiation emitted by the optical components, detector noise, amplifier noise and other system noise for internal electronic sources[16-20].

3. Development of Two-color RT

3.1 Optical system

The optical system (objective lens and detector) of the proposed two-color RT was selected according to the desired temperature measurement range, which is between 300 and 900°C. At the lower and upper limits of this temperature range (i.e., 300 and 900°C), the peak wavelengths of Planck's radiance are given as 2.3 and 5.1 μm, respectively.

The radiance and temperature are related in a nonlinear manner. To measure temperatures above 150°C and below the freezing temperature of silver (961.78°C), the wavelength of the employed detector should be shorter than the peak wavelength of Planck's radiances for the temperature of interest[16]. Accordingly, an uncoated infrared-grade calcium fluoride (CaF_2) lens and Hamamatsu two-color detector K11908-010K were selected to produce the optical system of the RT.

The CaF_2 lens has a diameter of 50.8 mm and possesses a high transmittance in the range from 0.3 to 5.5 μm. Also, CaF_2 lenses can endure temperatures of up to 800°C in dry environments. Furthermore, CaF_2 is inert when in contact with most acids, metal vapors, and gases.

The Hamamatsu two-color detector K11908-010K is composed of a short-wavelength (SW) InGaAs PIN photodiode mounted over a long-wavelength (LW) InGaAs PIN photodiode along the same optical path. The spectral responses of the SW and LW are 0.9 to 1.7 and 1.7 to 2.55 μm, respectively. The noise and dark current delivered by this detector is very low, and the K11908-010K detector allows for a simple probe design because only one optical path is required to simultaneously detect the thermal radiation at the two photodiodes. Also, this design decreases the attenuation caused by the optical filter that would otherwise be used to separate the thermal radiation into two spectral bands for two separate detectors.

3.2 Mechanical chopper

A mechanical chopper was employed to interrupt the incident radiation from the measured object to the detector. The chopper was mounted on a wind mill driven by supplied air. This technique was found to be more efficient than using an electric motor to rotate the mechanical chopper because using an electric motor can result in interference. Also, the supplied air was used to cool the detector to maintain the temperature within recommended values (i.e., -40 to +70°C). In addition, the supplied air was driven through a passage designed in the probe housing to generate an air flow in front of the objective lens and protect it from contamination, especially in a dusty measurement environment.

3.3 Probe housing

The internal probe housing was made from black anodized aluminum, and the objective lens, mechanical chopper, detector and wind mill were assembled together within. Black anodized aluminum is a low-refractive material that minimizes internal reflection and stray radiation that can become a secondary source of radiation. The outer housing of the two-color probe was made from steel to endure the harsh conditions. The final probe design is shown in Fig. 1.

3.4 Photocurrent preamplifier

The photocurrent generated by the detector is very small and needs to be amplified, so an SR570 low-noise current preamplifier was implemented. This amplifier possesses a wide dynamic range consisting of 28 gain levels from 1 pA/V to 1 mA/V. Also, all amplifier functions can be controlled through an RS-232 interface, facilitating the integration and opera-

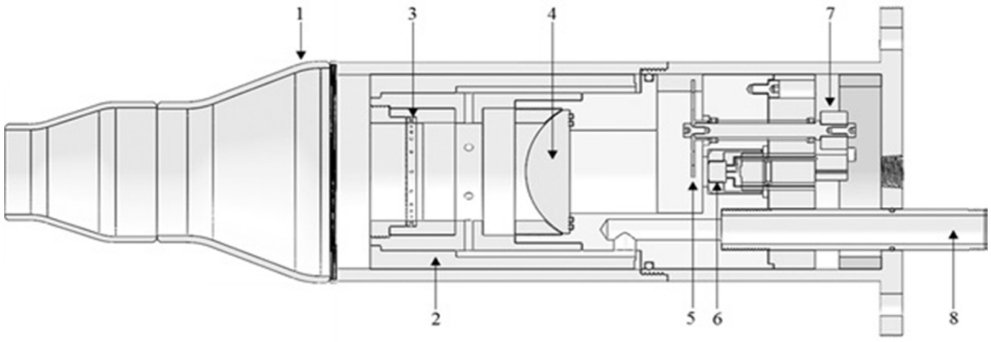

Fig. 1. Two-color probe: 1. Probe outer housing, 2. Probe inner housing (black anodized aluminum), 3. Honey comb, 4. Objective lens, 5. Mechanical chopper, 6. Two-color detector, 7. Wind mill, 8. Air supplying tube

tion of the amplifier with the other elements of the two-color RT.

3.5 Data Acquisition devices

Data was acquired with an NI 9222 data acquisition module and NI 9213 thermocouple module. Both modules were mounted on an NI cDAQ 9184 Ethernet chassis that was used to digitize the acquired analog data.

3.6 Data processing algorithm

The signal processing routines required for this application were developed using the Laboratory Virtual Instruments Engineering Workbench (LabVIEW) software. The routines were developed to:

i. Control the operation of different devices (amplifiers and data acquisition system).
ii. Perform signal-processing routines required to calculate the object temperature.

The sampling rate and sampling frequency of the data acquisition devices were optimized for the software to acquire data and transform it into a digital format.

A simple median filter was applied to remove the noise, and the signal base line was set to zero to facilitate signal intensity calculations. The validity of the signals was decided according to their intensity and width. Therefore, a wavelet of amplitude ranging from 0.01 to 5 V with a minimum width of 5 points was developed as reference for valid signals. The valid signals were normalized considering the gain level of the two amplifiers. The ratio, R, between the normalized signals was calculated and compared with the calibration curve obtained by the blackbody calibrator, and the object temperature was then calculated.

4. RT Measurements Experiments (Laboratory scale)

4.1 Two-color RT optical characteristics

The optical characteristics of the proposed two-color RT were studied using an OMEGA BB-4A Blackbody Calibrator. The two-color probe was perpendicularly placed 6 m from the blackbody calibrator, and a laser beam was used for alignment. The blackbody temperature was set to 200°C, and the frequency of the mechanical chopper was adjusted to approximately 50 rotations per second. The probe output, including the SW and LW band signals, was connected to the first and second amplifier using short coaxial cables to reduce excessive capacitance in the measurements, and the gain of the amplifiers were manually set. The amplified signals, $I_{\lambda 2}$ and $I_{\lambda 1}$, were acquired in the first and second channels of a Tektronix TDS2024C digital storage oscilloscope.

This procedure was repeated every 20°C from 200 to 900°C. The ratio ($I_{\lambda 2}/I_{\lambda 1}$) was calculated for each temperature, and the characteristics of the calibration curve were obtained by plotting the blackbody tem-

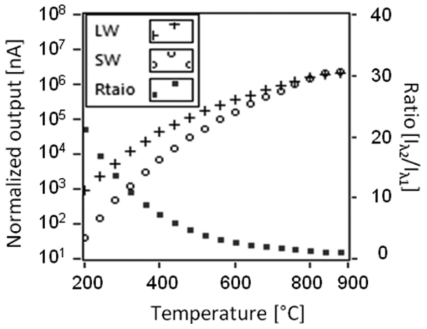

Fig. 2. Normalized output signals of the SW and LW channel ($I_{\lambda 1}$ and $I_{\lambda 2}$) and the ratio ($I_{\lambda 2}/I_{\lambda 1}$) as a function of the blackbody temperature

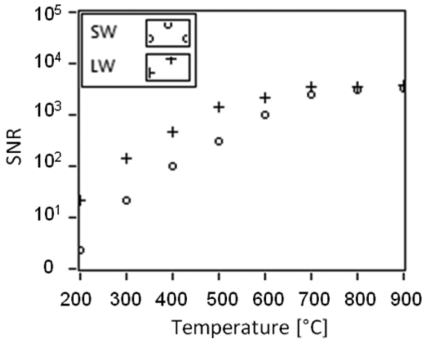

Fig. 3. SNR for the SW and LW channel as a function of the blackbody temperature

perature (T) versus the calculated ratio (R). The results are shown in Fig. 2.

The temperature as low as 200°C can be measured using the setup described above. The resulting signals were analyzed with the mean signal-to-noise ratio (SNR) calculated based on the ratio of the signal amplitude to the root mean square of the signal, and the mean SNR results are shown in Fig. 3.

The mean SNR calculated at the minimum measured temperature reached 2.3, and as the blackbody temperature increases, the mean SNR also increases for both SW and LW channel. The results of the mean SNR calculation were consistent with those presented by Hobbs *et al.*[31].

4.2 Radiation thermometry measurements for unknown emissivity object

To assess the performance of the proposed two-color RT, the blackbody calibrator was replaced with a test specimen consisting of a carbon steel plate of unknown emissivity with a diameter of 80 mm and thickness of 4 mm. The two-color probe was at a 6 m distance from the test plate. The plate was electrically heated and the back side of the plate was insulated with a ceramic fiber insulating material to stabilize the plate temperature. A solid state relay device (SSR) was used to set the plate temperature.

The setup used in Section 1 was used, except that the output of the two amplifiers was connected to the first and second channel, A0 and A1, of an NI 9222 module. Short coaxial cables were used to transfer the signal from the two-color detector to the amplifiers and from the amplifiers to the NI 9222 module. A K-type thermocouple of special limit of error of 1.1°C was attached to the center of the plate and was connected to the NI 9113 thermocouple module. Both modules were mounted in an NI cDAQ 9184 chassis connected to a computer through an Ethernet cable, and the computer was equipped with the LabVIEW software.

The RRS was set to 700°C, and the electric source was then turned on. When the plate temperature reached 700°C the electric power source was turned off and the plate was cooled down using a fan. The signals acquired from the two-color probe were processed in real time and stored. The plate temperature was simultaneously measured using the attached thermocouple, and the results were recorded. The temperature data obtained from the two-color RT were compared to that obtained from the thermocouple, and the difference between them was maintained within the temperature measurement error of the two-color RT.

5. Temperature Measurements Error Analysis

The radiation thermometry measurements were carried out in an ambient temperature of 23°C, and in such conditions, the measurement environment has a

negligible influence with the main error in the temperature measurement arising from the detector and amplifier noise.

The error in temperature measurements due to detector and amplifier noise is determined by applying the method described in Ref.[24,25]. This method calculates the temperature error from the ratio of the percentage error in the output signal amplitude to the percentage of change in the output signal due a change in the blackbody temperature of 1°C, which is the Percent-Per-Degree (PPD)[24,25].

The error in the output signal amplitude for each sensor was determined using the following formula:

$$\frac{(MA_{\max}-MA_{\min})/2}{MA_{mean}}\times 100 \quad (8)$$

where, $MA_{\max}$, $MA_{\min}$ and MA_{mean} were configured as shown in Fig. 4.

The PPD for each sensor was calculated as follows:

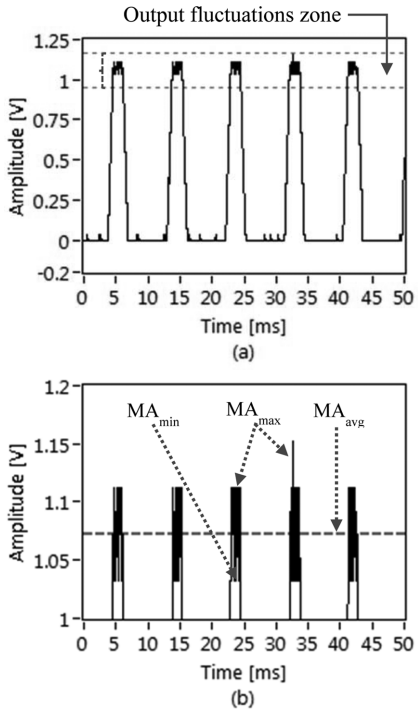

Fig. 4. Output voltage fluctuations during radiation thermometry measurements. (a) Raw signal, (b) Output voltage fluctuation zone

$$PPD(\%/^{\circ}\mathrm{C}) = \frac{c_2}{\lambda T^2}\times 100 \quad (9)$$

where λ isthe effective wavelength for each sensor, taken as the peak sensitivity wavelength given by the detector manufacturer.

At laboratory scale, the detector and amplifier are the dominant noise sources at a low temperature. As the temperature increases, the shot noise induced by the photocurrent generated from the detector becomes more significant.

When measuring at temperatures from 200 to 900°C, the temperature error ranges from 2.4 to 0.2°C for the SW channel as a single RT and ranges from 1.3 to 0.1°C for the LW channel. The temperature error that is calculated is larger relative to the temperature error resulting from the SW and LW channel as a single RT. These results are consistent with the fact that the error of a single-wavelength thermometer is smaller compared to two-color RT[22].

The proposed two-color RT is used to record plate temperatures of 200, 300 and 400°C with a temperature error of 6.1, 3.2 and 2.1°C, respectively. The temperature error from the ratio of the output error percentage and the PPD and that resulting from the two-color RT compared to the thermocouple were calculated and are shown in Fig. 5.

The acceptable temperature error is assumed to be 2°C, as is recommended for high quality infrared thermometry[26]. Regardless of the higher temperature

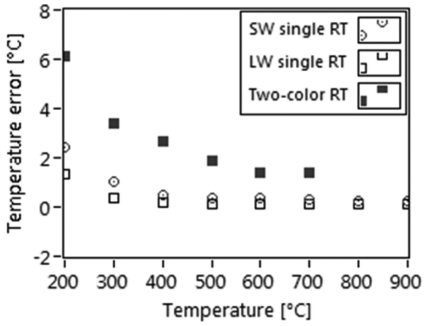

Fig. 5 Comparison of temperature error resulting from the SW and LW channel as a single RTs and that resulting resulting from the two-color radiation thermomeeter compared to a k-type thermocoupe

error in two-color RT compared to that for a single RT, the two-color RT has the advantage of being able to measure the temperature of the object without having previous knowledge of its emissivity. Also this error can be neglected when the two-color RT is used for temperature monitoring in industrial application in which the process is not influenced significantly by such temperature measurement errors.

6. Radiation Thermometry Measurements (Blast furnace)

The real-time performance of the proposed two-color RT by using it to monitor the temperature of the burden surface in a blast furnace used for pig iron production, which is considered as one of the harshest industrial environments. Monitoring the temperature of the burden surface in real time provides valuable information to operators because it has a direct relationship with the gas permeability and raw material feeding rates. Radiation thermometry measurements were performed and data was stored for a two-month duration. Fig. 6 shows the signal trend for 1 s.

The objective of this work is to obtain a temperature measurement every 33 ms, and the timing of the data acquisition system was optimized to this end. Fig. 7 shows the signals, calculated ratio, and temperature obtained during 33 ms.

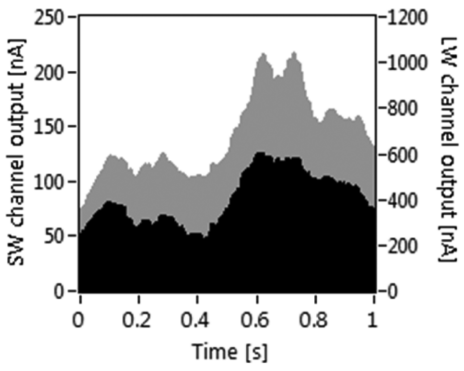

Fig. 6. Signals obtained from the SW band (black), and LW band (gray) channels during 1s

7. Temperature Correction Method

In ambient conditions in a laboratory, the transmittance of the SW and LW bands of the detector are assumed to be equal to each other. For a blast furnace, on the other hand, gases and dust are present in the field of view (FOV) of the RT. In such conditions, the thermal radiation emitted by the burden surface can be scattered and absorbed by the constituents of the measurement environment, resulting in a different transmittance for the SW and LW bands and thus leading to a significant error in the measured temperature. Therefore, a method was developed to determine the transmittance of the SW and LW band through the path between the burden surface and the two-color probe.

The effect of the absorption by the above burden gases and scattering by the fine dust particles were studied, and the transmittance of the SW and LW bands were determined as follows:

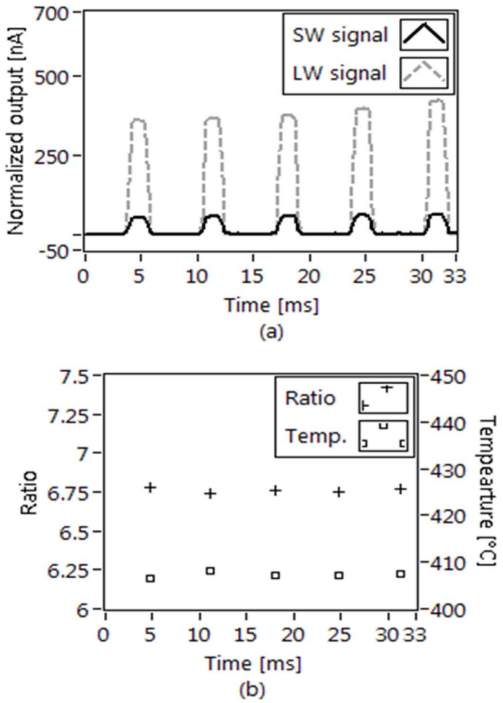

Fig. 7. (a) Signals obtained from the SW and LW band channel and (b) the ratio of the two signals and the calculated temperature during 33 ms

i. Transmittance of the SW and LW bands through above burden gases:

First, the absorbance of the SW and LW bands due to each gas fraction were calculated using the HITRAN code assuming a gas temperature of 300°C[27]. Each band was represented by an effective wavelength of $\Delta\lambda$ equal to 0.1 μm, and the central wavelength of each band is the peak sensitivity wavelength of the color band, in this case 1.55 and 2.1 μm for the SW and LW band, respectively.

The transmittance of the SW and LW bands for each gas fraction were calculated from the absorbance results using the following formula:

$$\text{Absorbance} = 2 - \text{Log}(\%\tau) \quad (10)$$

Then the effective transmittance of the medium, τ_0, was calculated based on the sum of the volume average transmittance of the gas/gas mixture in the medium, which is given as follows:

$$\tau_0 = \tau_1\upsilon_1 + \tau_2\upsilon_2 + \ldots + \tau_n\upsilon_n \quad (11)$$

where τ_1, τ_2……τ_n are the transmittance through different gas constituents, and υ_1, υ_2……υ_n correspond to the volume fractions of the different gas constituents.

Above burden gas is composed of 22 vol% CO_2, 23 vol% CO, 4.6 vol% H_2O and 44 vol% N_2[28]. Based on this method, the transmittance of the SW and LW bands through above burden gases were found to be 0.93 and 0.91, respectively.

ii. Transmittance of the SW and LW bands through above burden fine particles:

Coal particles are the main component of gas dust in a blast furnace. These particles form during the pulverized coal injection process (PCI)[29]. 5 kg of fine dust are collected in the dust catcher from 1 ton of iron ore, and coal particles ranging in size from 0.01 to 0.4 μm were characterized, revealing a mean particle diameter of 0.2 μm.

The total volume of the gases in the above burden zone is 449.4 m^3. Assuming that the density of the collected coal particles is 3.12 g/cm^3 and that the mean particle size is 0.2 μm, then the number of

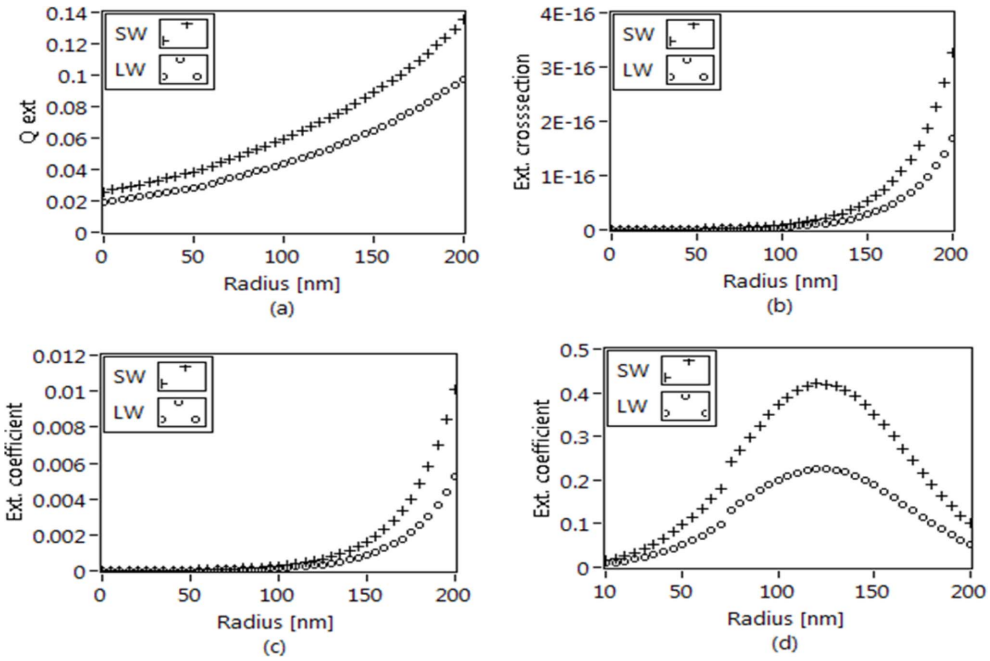

Fig. 8. (a) Extinction efficiency, Qext, (b) Effective extinction cross-section, σext, (c) Extinction coefficient, Cext, and (d) Extinction coefficient based on the coal particle distribution for the SW and LW bands

particles per cm^3 is approximately equal to 69×10^3 particles.

The size parameter, x, was determined based on the size of the coal particles as follows[30]:

$$x = \frac{\pi r m_0}{\lambda_0} \tag{12}$$

where, r is the radius of a single particle (assumed to be a sphere), λ_0 is the incident wavelength with respect to vacuum, and m_0 represents the refractive index of the surrounding medium.

The size parameter of the coal particles was found to be $0.01 < x < 10$, and so Mie theory was used to determine the extinction coefficients of the coal particles for the thermal radiance at SW and LW bands in the above burden zone.

The calculation of extinction coefficient in Mie theory can be summarized as follow:

(1) For a particle with radius r and refractive index of m_0, the scattering efficiency (Q_{sca}), absorption efficiency (Q_{abs}), and extinction efficiency (Q_{ext}), were calculated for the SW and LW band where Q_{ext} is equal to the summation of Q_{abs} and Q_{ext} (Q_{ext}, Q_{abs} and Q_{ext} are dimensionless)

(2) Then effective extinction cross-section (σ_{ext}) for each color band was calculated.

(3) Finally, the extinction coefficient (C_{ext}) is obtained by multiplying σ_{ext} by N, where N is the number of particles with radius r.

The results of the extinction coefficients calculations for the SW and LW band are shown in Fig. 8 below.

The objective of these calculations is to determine the transmittance of the SW and LW bands through the path between the burden surface and the two-color probe. Therefore, the Beers-Lambert law that describes the attenuation of radiation through the atmosphere was applied [31].

$$\tau_L = I/I_0 = e^{-C_{ext}L} \tag{13}$$

where τ_L is the transmittance of the medium, I is the measured intensity, I_0 is the initial intensity emitted by the object, C_{ext} is the total extinction coefficient, and L is the path length.

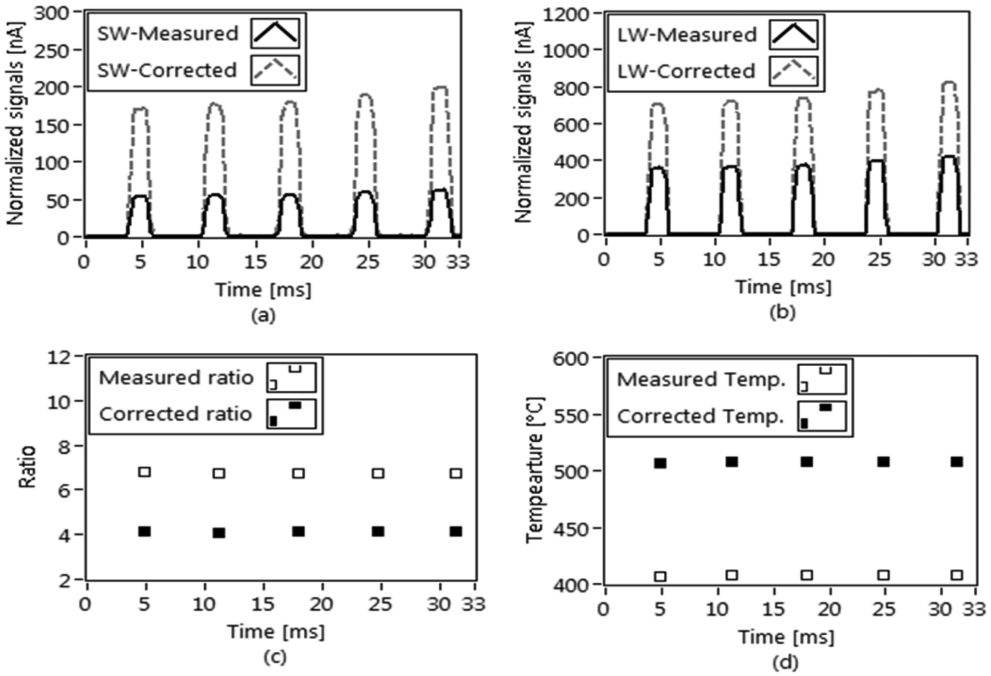

Fig. 9. Comparison between measured and corrected (a) Short wavelength band channel signal (b) Long wavelength band channel signal (c) Ratio (d) Temperature

Accordingly, the transmittance of the above burden zone of the BF was found to be 0.311 and 0.508 for the SW and LW bands, respectively. This result is consistent with the fact that long wavelengths suffer fewer atmospheric attenuation than short wavelengths[31,32].

The signal measured at the two color bands was corrected according to the values obtained for the above burden zone transmittance for the SW and LW bands to determine the true burden surface temperature, as shown in Fig. 9.

8. Conclusions

In this study, a real-time two-color RT was proposed as a viable device to measure temperature in harsh environments. The RT has a simple, compact probe design that is combined with a powerful data acquisition system and efficient LabVIEW code. As a result, the developed two-color RT can take reliable measurements of temperature ranging from 300 to 900°C in harsh environments, with long-term durability and stability.

The efficient LabVIEW software was developed to harmonize the operation of the different elements and to execute the signal processing routines and calculations required by this application.

In ambient conditions in a laboratory, the measurement environment has negligible effect, and the error in the measured temperature is mostly due to detector and photocurrent amplifier noise. The error obtained when comparing the temperature obtained by the proposed two-color RT to that obtained by a k-type thermocouple readouts was determiend to be within 6.1 to 1.4°C for the temperature range from 200 to 700°C.

Acknowledgements

The authors would like to acknowledge the Regional Innovation Center at Chonnam National University (Yeosu Campus) for supporting this work.

References

(1) Hollandt, J., Hartmann, J., Struß, O., and Gärtner, R., “Industrial applications of radiation thermometry”, Experimental Methods in the Physical Sciences, Vol. 43, 2010, pp. 1-56.
(2) Zhang, Y., “Novel optical sensors for high temperature measurement in harsh environments”, PhD dissertation. Faculty of the Virginia Polytechnic Institute, 2003.
(3) Hastie, J. W., Plante, E. R., and Bonnell, D. W., ACS Symposium Series, Vol. 179, 1982, pp. 543-600.
(4) Werner, M. and Fahrner, W., IEEE Trans. Ind. Electron., Vol. 48, No. 2, 2001, pp. 249-257.
(5) Leigh, J. R, “Temperature measurement & control. London”, U.K.: P. Peregrinus on behalf of the Institution of Electrical Engineers, 1988.
(6) Lu, G., Yan, Y., Riley, G., and Bheemul, H., IEEE Trans. Instrum. Meas., Vol. 51, No. 5, 2002, pp. 990-995.
(7) Castrellon-Uribe, J., Paez, G., and Strojnik, M., “Infrared Spaceborne Remote Sensing IX”, 2002, doi: 10.1117/12.455137.
(8) Koo, K. M., Kim, J. H., Kim, S. B., Kim, H. D., and Ko, D. Y., Proc. IECIC, 2001, pp. 229-232.
(9) DeWitt, D. P. and Nutter, G. D., “Theory and Practice of Radiation Thermometry”, Wiley, 1988.
(10) Magunov, A. N., Instruments and Experimental Techniques, Vol. 52, No. 4, 2009, pp. 451-472.
(11) Magunov, A. N., Pylnev, M. A., and Lapshinov, B. A., Instruments and Experimental Techniques, Vol. 57, No. 1, 2014, pp. 86-90.
(12) Zhang, Z. M. and Lee, B. J., “Theory of Thermal Radiation and Radiative Properties”, Experimental Methods in the Physical Sciences, Vol. 42, 2009, pp. 73-5132.
(13) Planck. M., Ann. der Phys., Vol. 4, 1901, pp. 553-560.
(14) Müller, B. and Renz, U., Rev. Sci. Instrum., Vol. 72, No. 8, 2001, pp. 3366-3374.
(15) Coates, P. B., Metrologia, Vol. 17, No 3, 1981, pp. 103–109.
(16) Madruga, F. J., González, D. A., and López-Higuera, J. M., IEEE Sens. J. A, Vol. 4, No. 3, 2004, pp. 288-294.
(17) Zhang, Z. M. and Machin, G., “Overview of radiation thermometry”, Experimental Methods in the Physical Sciences, Vol. 42, 2009, pp. 1-28.
(18) Chrzanowski, K., Appl. Opt., Vol. 34, No. 16, 1995, pp. 2888-2897.

(19) Chrzanowski, K., Appl. Opt., 1996, Vol. 35, No. 19, pp. 3540-3547.
(20) Fehribach, J. D. and Johnson, R. B., Opt. Eng, Vol. 28, No. 12, 1989, pp. 1255-1259.
(21) Neuer, G., Fiessler, L., Groll, M., and Schreiber, E., "Critical Analysis of the Different Methods of Multi-wavelength Pyrometry", In Schooley, J. F. (Eds.), Temperature: Its Measurement and Control in Science and Industry, AIP Press, 1993.
(22) Taylor, J., Foundation Level Infrared Training, 2010.
(23) Machin, G. and Chu, B., Imaging Sci., Vol. 48, 2000, pp. 15-22.
(24) Xinxin Zhou, Matthew J. Hobbs, Benjamin S. White, John P. R. David, Jon R. Willmott, and Chee Hing Tan, IEEE Trans. Electron. Devices,, Vol. 61, No. 3, 2014, pp. 838-843.
(25) Matthew J. Hobbs, Chee Hing Tan, Xinxin Zhou, John P. R. David, Jon R. Willmott, Elena Plis, and Sanjay Krishna., IEEE Trans. Instrum. Meas., 2015, Vol. 64, No. 2, p. 502-508.
(26) Quinn, T. J., Temperature, London: Academic Press, 1990.
(27) Lumina Labs, SpectraPlot, http://www.spectraplot.com/absorption.
(28) Lundgren, M., "Blast Furnace Coke Properties and the Influence on Off-gas Dust", Licentiate thesis, Luleå University of Technology, 2010.
(29) Das, B., Prakash, S., Reddy, P., and Misra, V., Resources, Conservation and Recycling, 2007, Vol. 50, No. 1, pp. 40-57.
(30) Wallace, J. M., and Hobbs, P. V., "Atmospheric Science: An Introductory Survey", Orlando: Academic Press, 1977.
(31) Weichel, H., "Laser beam propagation in the atmosphere, Bellingham", WA, USA: SPIE Optical Engineering Press, 1990.
(32) Pratt, W. K., "Laser communication systems", New York: Wiley, 1969.